Nuclear Engineering and Design/Fusion 4 (1987) 149–163
North-Holland, Amsterdam

CRYOPUMPING FOR FUSION REACTORS

Douglas W. SEDGLEY and Albert G. TOBIN

Grumman Aerospace Corporation, Bethpage, New York 11714, USA

Thomas H. BATZER and Wayne R. CALL

Lawrence Livermore National Laboratory, Livermore, California, USA

Received October 1985

Fusion reactors will exhaust large volumes of hydrogen species and helium, and cryopumps can satisfy the pumping needs. Two programs described here were undertaken to develop the high performance, continuous operation required. The capability of charcoal as a cryogenic sorbent was optimized and improved by use of specific charcoal types and grades, and by use of thermally conductive bonds for attaching the charcoal to the cryogenically cooled substrate. A 30% demonstrated pumping speed improvement is significant for a system in which the pump dimensions are measured in tens of square meters.

An automatically controlled continuous duty cryopump system was developed, fabricated and demonstrated. The system pumps deuterium, and can be readily modified to pump helium by addition of a sorbent such as charcoal. This two-unit system has one unit being regenerated while the other unit is pumping. It is prototypical of a fusion reactor pump in which five units would be pumping for each unit that is being regenerated. Low tritium holdup is projected for an operational installation.

1. Introduction

Fusion power reactors and fusion experiments leading to commercialization of fusion power will discharge large volumes of gas, principally hydrogen isotopes and helium. Helium, the product of the fusion reaction, is produced at a rate of more than 10 Torr-*l*/s for every 1000 MW of fusion power. The amount of deuterium and tritium (D–T) to be pumped depends on the efficiencies of the fusion process (fractional burnup) and of the particle injection devices. D–T in quantities up to ten times the helium quantity might have to be pumped in a power reactor.

The high vacuum pump types most frequently cited for fusion applications are the turbomolecular pump and the cryopump. Diffusion pumps, which also pump helium and hydrogen isotopes effectively, are generally discounted because of the use of oil as a working gas, with the potential of reactor vessel contamination. Turbomolecular pumps (TMPs) have found application in fusion experimental devices and studies, but are generally applied where the speed requirements are low. TMPs with speeds up to 50,000 *l*/s helium are projected by Perenic [1], although currently the largest models are in the range below 7000 *l*/s. Cryopumps have the capability of being shaped to fit the installation, and their total pumping speed is limited only by their size. Helium speeds in the range of 2 to 4 *l*/s for each cm^2 of pumping surface have been demonstrated for thermally shielded pumps by Batzer [2], Hseuh [3] and Anderson [4]. Section 2.2 predicts the potential for improvement.

The choice of TMPs may be based on a perceived advantage of operational simplicity, however the convenience of continuous duty cryopump operation has been demonstrated. Tritium holdup in a cryopump system is acceptably low. Cryopumps offer the advantage of configurational flexibility, particularly as size is increased to satisfy high pumping speed requirements.

Considering the requirement to dispose of the helium exhaust, fig. 1 shows for a typical reactor what the options may be. Tokamak reactors (such as STARFIRE [5]) use appendage-type pumping because of space restrictions around the torus. The intervening duct system between the pump and the torus is an impedence to flow. The more restrictive this impedence becomes, the greater the pump speed S_p has to be compared to the effective speed S_{eff}, which is the speed at the vacuum vessel/vacuum system interface. A ratio of S_p/S_{eff} equal

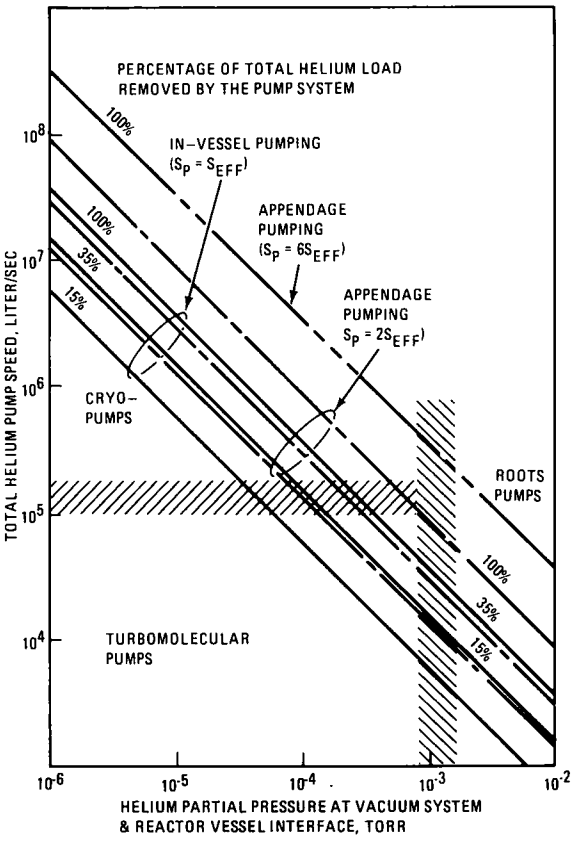

Fig. 1. Helium pumping requirement for a 3500 MW reactor.

to six is representative of a tokamak because of the space restrictions for pumping. The particle diverter methods currently favored are the pumped limiter and magnetic diverter, e.g. by Conn [6] and Post [7]. Either device is effectively a compression stage which raises the pressure of the neutralized ions within the limiter, with the consequence of lowering the pumping speed requirements. A ratio S_p/S_{eff} of two is appropriate for the more accessible mirror reactor installation.

Mirror reactors (such as MARS [8]) have either in-vessel helium pumps or a combination of in-vessel and appendage pumps. Current theory projects the ability to direct most of the helium to the plasma edge region (halo region). Helium trapped in the halo plasma follows the field lines into the end tanks and is compressed in the halo scraper, which is configurationally similar to the pumped limiter. An appendage pumping system is attached to the halo scraper. A portion of all helium, however, specifically that born in the loss cones, remains in the main cavity of each end tank and is pumped on in-vessel pumps.

Each curve in fig. 1 represents a constant throughput of helium, with the percentages representing the portion of the total throughput handled by the pump system. In tokamak reactors, 100% of the helium is pumped through an appendage system typically represented by the upper curve. In mirrors the helium pumpout may be split between an appendage pumping system and in-vessel system as mentioned previously. For the in-vessel system the pump total pressure is equal to the reactor end tank plasma pressure which is on the order of 2×10^{-5} Torr. The corresponding helium partial pressure ranges from about 5×10^{-6} to 10^{-5} Torr depending upon the fuel fractional burnup ratio. So that, even if the percentage of helium captured on the in-vessel pumping system were as low as 15%, cryopumps are the preferred choice. The choice for appendage pump type is less clear because the capability of the halo scraper (or pumped limiter) to compress the edge plasma pressure is not fully defined. Although experiments, e.g. by Jacobson [9] have shown good compression in limiter-type probes, scaling to reactor conditions is not certain. The best that can be said today before development of large TMPs is this: Tokamaks, which produced helium partial pressures in the limiter lower than 10^{-3} Torr probably will require cryopumps. For mirrors, which requires above about 10^{-4} Torr partial pressure in the scraper to make TMP's (or blowers) practical, the choice is less certain. In-vessel units will likely be cryopumps.

It appears likely that cryopumps will be required for a fusion reactor of either the tokamak or mirror configuration, thus it is appropriate to pursue cryopump technology issues. High pumping speed requirements mandate the need to improve pumping efficiency.

2. The fusion cryopump

The fusion cryopump is so-named because it is compatible with the fusion environment and can pump by cryogenic condensation or sorption, all gases from the fusion reactor chamber, principally helium and deuterium–tritium (D–T). Trace amounts of condensible impurity elements and compounds are also pumped. The cryopump is a candidate for both tokamak and mirror fusion reactors as noted previously because of its configuration flexibility and its high pumping speed.

2.1. Elements of a fusion cryopump

The basic gas handling elements of a fusion cryopump are shown in fig. 2. Although not all items are required for all pump concepts as is noted below, those

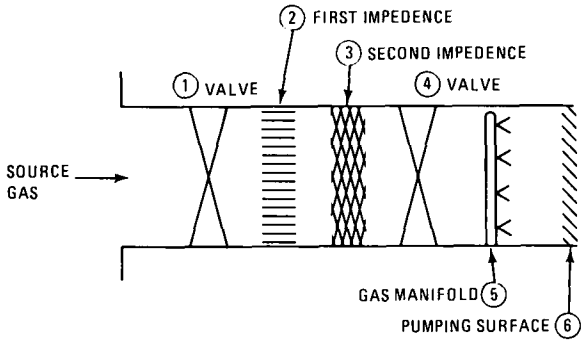

Fig. 2. Schematic of a cryopump showing the elements which affect pump speed.

that are place between the pump's inlet and the pumping surface reduce its speed and provide the incentive to improve particle capture efficiency of the surface.

(1) This valve or movable baffle provides the means of isolating the inner surfaces of the pump from the gas particle source. When it is in the closed position, the pumped particles can be degassed and disposed of without reintroducing them to the vessel being pumped.

(2) This optically opaque shield, conveniently maintained at approximately 77 K by liquid nitrogen coolant, greatly reduces the thermal radiation load on surfaces within the pump being held at temperature in the range of 4 K. Item 2 is a necessary element which, however, contributes to reducing the helium effective pumping speed.

(3) This intermediate, optically opaque surface is included in a pump design to condense gas particles other than helium. Inclusion of this pumping surface effects separation of all other fusion exhaust constituents from the helium. This separation may be done to allow independent degassing and disposal of the helium, and/or to prevent the other constituents from reducing the helium pumping speed if they are pumped on a common surface.

(4) This door, valve, or conductance-limiter is only used in concert with item, 3 and if needed provides the means of separately degassing item 3 and item 6. It may be feasible to separately degas these items without requiring this conductance limited in the design, by proper sequencing of the regeneration process.

(5) This gas manifold provides the working gas which is sprayed toward the inner pumping panel (Item 6), freezes and adsorbs the pumped gas. This manifold is used in conjunction with a smooth surface pumping panel on which helium cannot otherwise by cryocondensed. It is not required if the pumping panel surface is coated with an appropriate solid sorbent material. The manifold is maintained at a temperature above the ambient freezing point of the working gas.

(6) This panel is the helium pumping stage of the cryopump. It is cooled to a temperature at or below the ambient boiling temperature of liquid helium, and captures helium by cryosorption either in a solid sorbent or by trapping with a working gas.

The fusion cryopump is an element of the on-site fusion fuel cycle. The cycle comprises the subsystems for tritium handling, breeding, dissociation, separation, storage and reinjection. The design of the cryopump is inseparable from the design of the fuel cycle components. The pump ultimately passes the reactor gases on for cleanup, dissociation, and disposal or reuse. The question is where in the cycle the separation of gases should take place. Can the helium be separated from the D–T in the cleanup system or should it be separated out in the pump? Helium separation cannot be effected in a TMP and selection of this pump type would mandate helium separation elsewhere in the fuel cycle.

The present Tritium Systems Test Assembly (TSTA) at Los Alamos National Laboratory (LANL) which is prototypical of an on-site fuel cycle, separates helium from D–T in the vacuum pumping system, described by Coffin [10], specifically in a compound cryopump. This compound concept may be the appropriate arrangement, namely to capture D–T and other condensibles on one surface (Item 3 above) and the helium on another (Item 6), so that helium can be separately disposed of without passing it through the cleanup system. A couple of disadvantages can be cited: The additional surface is a conductance barrier which reduces helium pumping speed; and the time required to degas helium and D–T in series increases tritium holdup in the vacuum system. The latter problem can be diminished by placing a valve or barrier (Item 4) between the two surfaces [10], which will allow concurrent degassing.

An alternative may be to pump all gases on a single surface with the requirement to separate them elsewhere. The potential is for improved conductance and therefore reduced pumping system size, which for a pumping system whose dimensions are measured in tens of square meters is worth assessing. The gain in conduction however may be offset by the reduction in cryopanel capture coefficient from copumping as shown by Hseuh [3].

2.2. Speed of a baffled cryopump

The theoretical specific pumping speed S_{ideal} for an

unbaffled surface with no accumulation is

$$S_{\text{ideal}} = 3.638\,(T/M)^{1/2} \quad [l\ \text{s}^{-1}\,\text{cm}^{-2}], \tag{1}$$

where T is the temperature (K) of the pumped particles with molecular weight M. For a real installation the specific pumping speed is $S_p = kS_{\text{ideal}}$, where k is a complex function of the pump geometry accounting for the effect of baffles, and of the particle capture coefficient. The helium/hydrogen cryopump has most or all the items described above. The expression for k for several impedences in series from O'Hanlon [11] is

$$1/k = 1/k_1 + 1/k_2 + \ldots + 1/k_n - (n-1). \tag{2}$$

Specific pumping speed for a pump with two baffles, in which the baffle areas and the pumping surface areas are equal, is

$$S = S_{\text{ideal}}(1/t_1 + 1/t_2 + 1/c - 2)^{-1} \quad [l\ \text{s}^{-1}\,\text{cm}^{-2}], \tag{3}$$

where t is the transmissivity of an impedence (Item 2 and 3) and c is the capture coefficient of the pumping surface (Item 6). Transmissivities of 0.27 and 0.45 for a chevron baffle and a louver baffle respectively are used based on data by Santeler [12] to predict helium pumping for a two-chevron pump of 4.9 $l\ \text{s}^{-1}\,\text{cm}^{-2}$ and for a louver-chevron pump 6.4 $l\ \text{s}^{-1}\,\text{cm}^{-2}$, assuming a capture coefficient $c = 1$.

3. Evaluation of charcoal sorbents

Anderson [4] tested as part of the Tritium Systems Test Assembly program, three cryopumps which featured (1) cryotrapping of helium using argon gas as a working fluid, (2) cryosorbing of helium using molecular sieve 5A, and (3) cryosorbing of helium using activated charcoal. Each pump had a double impedence. The argon pump's outer baffle was a louver, whereas all other impedences were chevrons. The outer impedence of each pump was liquid nitrogen-cooled to intercept gradient energy from the vacuum container walls. The inner impedence was cooled by liquid helium to intercept all gases except helium. Initial helium pumping speeds (no accumulation) for the three pumps were 2.0 $l\ \text{s}^{-1}\,\text{cm}^{-2}$ for the argon and charcoal pumps, and 1.0 $l\ \text{s}^{-1}\,\text{cm}^{-2}$ for the molecular sieve pump. Although none of these pumps had to be optimized for the TSTA application, the low performance of this latter pump was in general agreement with results by Fisher [13], and further evaluation of molecular sieve 5A as a cryosorbent to improve performance of the argon cryotrapping concept. Sedgley et al. [15] undertook a program described here to assess methods of improving charcoal as a cryosorbent of helium.

At the outset of this charcoal sorbent evaluation program, the use of charcoal as an alternative for cryopumping helium was no longer being pursued. It was felt that this methods could be improved significantly within the limites of fusion compatibility by improving the charcoal coverage on the pumping surface. Chemical bonding of charcoal with epoxy is commonly used in commercial applications, however use of epoxy resin binders is questionable in the fusion radiation environment. Hseuh [3] designed a compatible pump which featured mechanical bonding of charcoal with a solder, and this was the pump tested in TSTA. Solder bonding by its nature precludes high density coverage of sorbent, so other methods were considered including compatible cements and brazes, and mechanical attachments.

The resulting program was a limited test series which none-the-less produced means of improving the capability of charcoal for pumping helium for fusion application. The information derived from this work included the effect on helium pumping performance of:

- Charcoal type, size and mixture
- Charcoal retention
  - braze type and processing
  - mechanical attachment of sorbent
  - inorganic cements
- Contamination

The vacuum test installation shown schematically in fig. 3 is in the Lawrence Livermore National Laboratory (LLNL) Vacuum Technology Laboratory and was used for all performance tests. The test cryopump, within which charcoal, bond and substrate samples were placed, is a rugged pump designed by Livermore for ready demounting and servicing. Test samples consisted of 4-inch (10.2 cm) diameter discs which attached to the pump's liquid helium dewar. A liquid nitrogen-cooled chevron array shielding the helium dewar had an area that was significantly larger than that of the test discs ($> 30\times$), so that a correlation of results with eq. (3) (equal pumping surface and impedence areas) was not attempted. Instead a consistent set of procedures was followed with the same constant helium throughput (6×10^{-4} Torr $l\ \text{s}^{-1}\,\text{cm}^{-2}$) applied to almost all sample discs. The performance of the charcoal discs was compared to a "standard", comprising charcoal attached by an epoxy bond to an aluminium substrate, which although it is not a fusion-compatible assembly, has demonstrated good performance [3] and is appropriate for comparison.

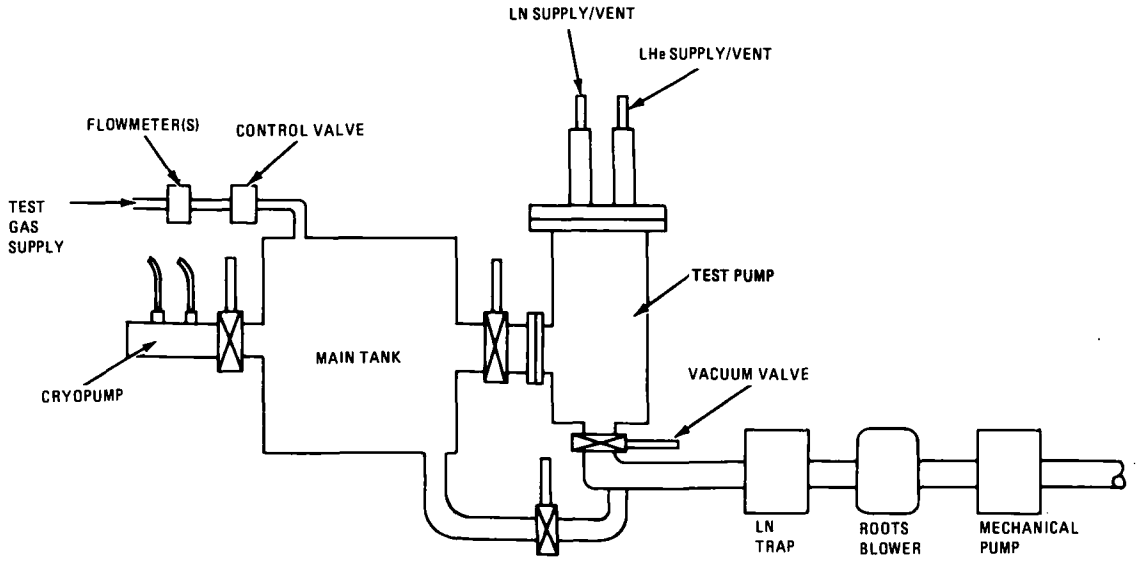

Fig. 3. Test system schematic – Charcoal samples are attached to the LHe dewar of the test pump.

3.1. Survey of charcoals

The survey looked at three charcoal grades; a coconut-based (PCB) * and a coal-based (BPL) * charcoal which were available as irregular particles, and another coal-based charcoal ** which was pelletized (fig. 4). When the charcoals were attached to a sticky surface to determine areal density (mass of charcoal per unit substrate area), the largest particle size surveyed (4×10 mesh) yielded the highest density (fig. 5). One might anticipate a direct correlation between helium pumping speed and pore area per unit substrate area, so that the largest PCB and BPL charcoals and the pelletized charcoal would perform well. This was not the case and in fact the larger particle sizes yielded low performance (figs. 6 and 7). It would be difficult to perform experiments to identify the precise reasons for this observation, however, it is suggested that the temperature of the smaller particle more closely approached the liquid helium temperature than the large ones. Given the measured sensitivity of helium pumping speed to charcoal temperature, a significantly larger portion of each smaller particle is available to pump helium.

Because the results shown above suggest that even

* Calgon Corp. Pittsburgh, Pa, USA.

** Desorex from Lurgi-Umwelt, Frankfurt, Fed. Rep. Germany.

TYPE	SOURCE	PORE DIAMETER, (Å)	PORE SURFACE AREA(m^2/g)	BULK DENSITY (g/cc)	PARTICLE DENSITY* (g/cc)	MESH SIZE (US SIEVE)
PCB	COCONUT	15-400	1150-1250	0.44	0.85	4x10 6x16 12x30 30x140 <325
BPL	COAL	15-400	1050-1150	0.48	.085	4x10 6x16 12x30
DESOREX**	COAL		1300	0.40		2 mm DIA x 7 mm CYLINDER

*Hg DISPLACEMENT
**PROVIDED BY LURGI-UMWELT, FRANKFURT, GOR
R85-1099-004B

Fig. 4. Description of as delivered charcoal grades.

CHARCOAL TYPE	PARTICLE SIZE	AREAL DENSITY (mg/mm^2)	PORE AREA/ SUBSTRATE AREA m^2/mm^2
PCB	(4x10)	1.225	1.4 -1.5
PCB	(6x16)	0.634	.73 - .79
PCB	(12x30)	0.347	.40 - .43
BPL	(4x10)	1.279	1.3 -1.5
BPL	(6x16)	1.063	1.1 -1.2
BPL	(12x30)	0.394	.41 - .45
DESOREX	–	1.067	1.4

R85-1541-001B

Fig. 5. Areal densities of charcoals (pure materials) on adhesive tape.

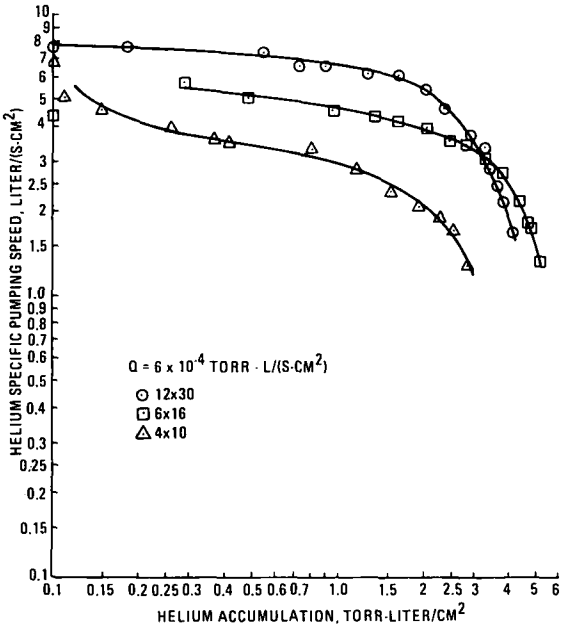

Fig. 6. PCB charcoal on epoxy bond – Comparison of different particle sizes.

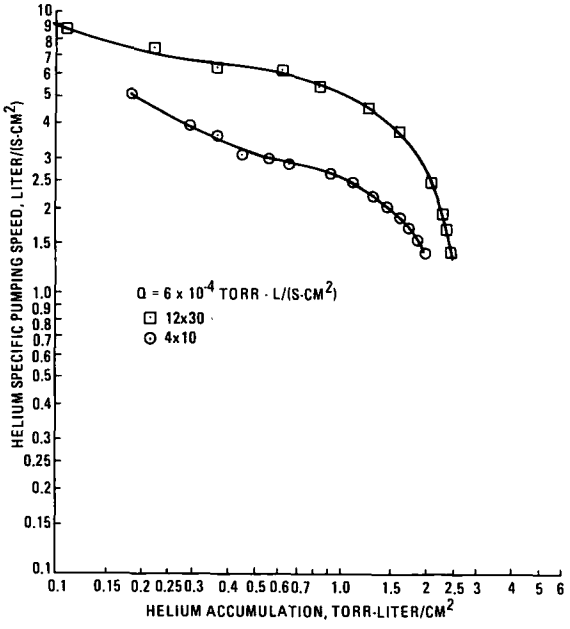

Fig. 7. BPL charcoal on epoxy bond – Comparison of different particle sizes.

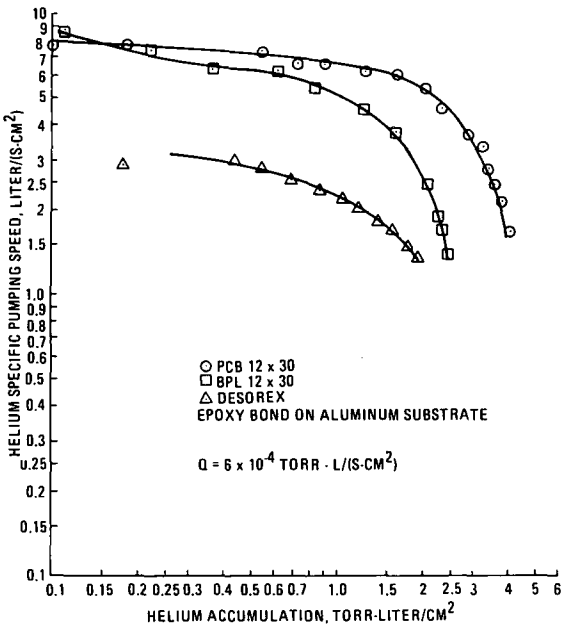

Fig. 8. Comparison of various charcoal types.

smaller sizes of charcoal may exhibit better performance, the tests were extended to include PCB granules in the size range of 30×140 mesh and < 325 mesh. Accumulation of helium on the 30×140 mesh samples was less than 0.3 Torr-l cm^{-2} when the vacuum tank pressure rose excessively, requiring run termination. Evidently the quantity of 30×140 mesh charcoal per unit area of substrate surface is insufficient to absorb the helium at the test flow rate. Consequently the finer mesh (< 325) was not tested. Within the scope of the survey, that is for helium specific throughputs representative of fusion reactor rates, the 12×30 mesh charcoal size is optimum for helium cryopumping.

Fig. 8 compares the best performing (12×30 mesh) coal and coconut charcoals to each other and to the pelletized charcoal. This limited evaluation showed that the coconut has a decided advantage over the other grades of charcoal in this application; all tests subsequently made and described below used the 12×30 mesh size coconut charcoal.

3.2. Charcoal bonding and retention studies

The particle size and grade tests described above used a silver-based epoxy bonding agent, and the highest performing sample (fig. 6) became the "standard" against which all subsequent performance runs were

compared. For reference, this standard sample pumped 7.8 $l\ s^{-1}\ cm^{-2}$ at low capacity and maintained above 7.1 $l\ s^{-1}\ cm^{-2}$ for approximately 20 min with the constant test flow of 6×10^{-4} Torr $l\ s^{-1}\ cm^{-2}$ helium.

Because the fusion neutron environment and tritium eventually degrade organic bonds, several approaches to achieving a thermally conductive bond using inorganic bonding agents were evaluated, including mechanical attachment, low temperature curing ceramic adhesives, low temperature curing metallic adhesives, and brazes.

A mechanical attachment method, in which charcoal was tamped into a titanium honeycomb attached to an aluminium substrate, and held by an 20 mesh screen, did not cryopump helium. The increased pore area of this arrangement was more than offset by the lack of thermal contact between the charcoal and the helium-cooled substrate.

Ceramic bonding agents based upon ZrO_2 and Al_2O_3, and metallic bonding agents based upon stainless steel and copper, were applied to metal substrates. Fig. 9 shows the results of testing these samples. The charcoal/copper cement sample produced satisfactory performance and showed that a useful inorganic bonding material was available for fusion application. (Subsequent development of improved methods increased this performance). Other samples in this category produced poor performance indicating the importance of good thermal properties of the bonding material; the sample using ZrO_2 as binder produced no helium cryopumping.

Commercially available silver-based braze alloys were surveyed for use as bonding agents. One method used a titanium wetting agent with the braze and produced well bonded charcoal particles. However, a look at the charcoal/alloy interface showed that the braze had infiltrated the charcoal pores. Cryopumping with this assembly produced low helium pumping performance (fig. 10). Possible contributing factors were the braze penetration, and/or exposure of the charcoal to 1175 K temperature during vacuum brazing cycle. To test the latter hypothesis, charcoal as heated to 1175 K then cooled and epoxy-bonded to a substrate. The sample's performance improved compared to the braze-bonded sample, but was considerably poorer than that of the "standard" sample. Baking the charcoal thus showed an adverse effect which was subsequently avoided by use of air-brazing methods.

Four brazes (fig. 11) were used for air-brazing charcoal to the substrate. The charcoal was partially embedded into the molten braze to effect the attachment and thus was not exposed to the high temperature cycle as in the case of the vacuum brazed sample. The silver-

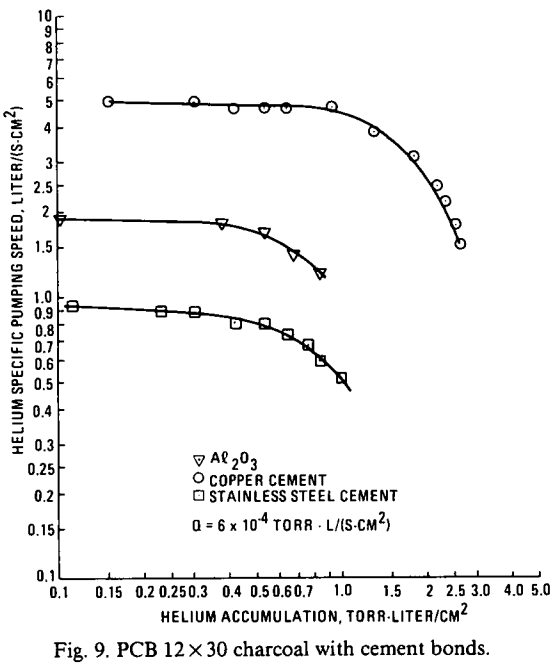

Fig. 9. PCB 12×30 charcoal with cement bonds.

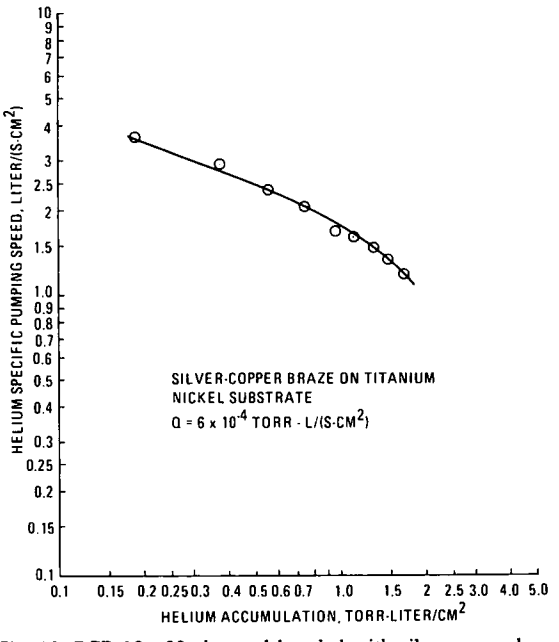

Fig. 10. PCB 12×30 charcoal bonded with silvercopper braze on titanium.

DESIGNATION	COMPOSITION, WT% Ag	Cu	OTHER	SOLIDUS (°C)	LIQUIDUS (°C)
AgCuP	15	80	5 P	640	705
BRAZE 495	49	16	23 Zn, 7.5 Mn, 4.5 Ni	625	705
BRAZE 852	85		15 Mn	960	970
HI-TEMP 095		52.5	9.5 Ni, 38 Mn	880	925

R85-1099-011B

Fig. 11. Braze alloy compositions evaluated for compatibility with charcoal.

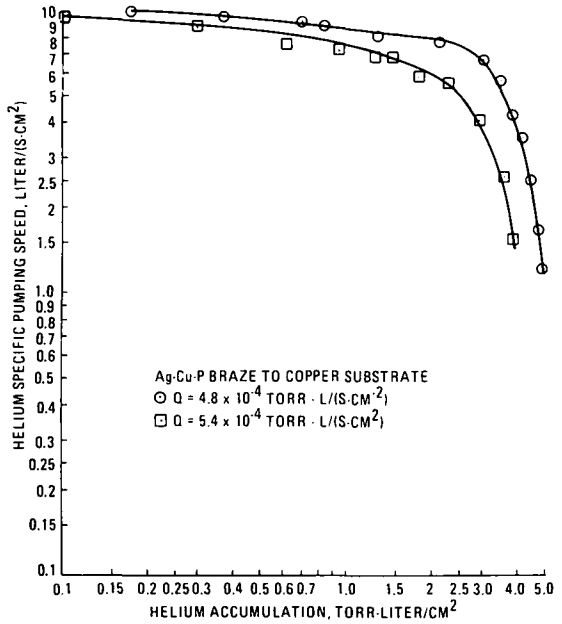

Fig. 12. PCB 12×30 charcoal – AgCuP braze to copper.

copper-phosphorous braze alloy, Sil-Fos * which is self fluxing yielded an effective bond. The other three brazes containing Mn, selected for their possible carbide-forming capability, oxidized severely and failed to bond the charcoal. Coconut charcoal attached by the AgCuP braze yielded helium pumping performance (fig. 12) superior to the epoxy "standard" and thus offered a fusion-compatible helium cryopump with a 30% performance improvement.

* Handy and Harmon, New York, N.Y.

3.3. Optimization of the bond

The copper cement bond and the AgCuP braze were evaluated further to optimize for improved performance and to determine bond integrity during thermal cycle tests consisting of transitions between 4.2 K and 40–85 K. The charcoal was attached using braze with thicknesses of 0.008 cm, 0.015 cm and 0.023 cm. Copper cements were used in as-received and in diluted forms. The charcoal attached using the 0.015 cm thick braze produced the best overall helium pumping performance in all three tests and was superior to previously described helium performance tests. Performance of the charcoal using the thinnest braze (0.008 cm) was comparable to the 0.016 cm bond; however the thickest braze caused the charcoal to shear at the bondline during cooldown due to thermal expansion mismatch, and the concomitant charcoal loss adversely affected performance. All samples completed the thermal cycle to LN temperature without loss of charcoal from the surface.

A diluted copper cement produced good charcoal retention, and the assembly pumped helium at the same high rate as the best braze-bonded sample (fig. 13). Variations in the cement dilution ratios yielded helium pumping performances with measurably lower pumping speeds. Because the study of the copper bond was less complete than that of the brazes, a braze bonded assembly using AgCuP braze was selected for preparation of a pumping panel for the (TSTA) Tritium Systems Test Assembly compound cryopump [4].

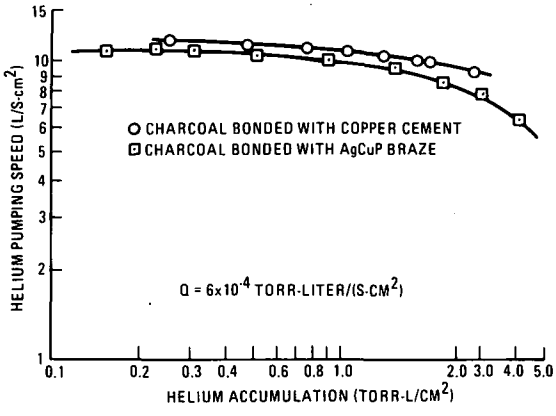

Fig. 13. Optimized performance of as-received PCB coconut charcoal 12×30 mesh.

3.4. Scale-up of an optimized bond for TSTA

A 40.6 cm diameter charcoal cryopanel was made up for testing on TSTA at the Los Alamos National Laboratory. The panel comprised nine roughly equal area tiles of copper substrate, AgCuP braze alloy bond and 12 × 30 mesh PCB coconut charcoal. The tile size picked was limited by available brazing facilities. Before delivery to Los Alamos the panel was pretested at Livermore by attaching it to its helium dewar (fig. 14) and mounting it in an LN-lined vacuum chamber. Fig. 14 shows also the LANL pump in exploded view. Fig. 15 shows the scaled-up panel's indicated pumping performance based on a helium throughput of 6×10^{-4} Torr $l\ s^{-1}\ cm^{-2}$ as for the smaller samples, and on the reading of a nude ionization gage mounted in the cold space between the LN-cooled shield and the pump's dewar.

The speed of cryopump units with a two-chevron baffle with the optimized charcoal panel can be projected from the test data using the following correlation:

$$S_{WB} = t\, S_{WOB}, \tag{4}$$

where S_{WB} is the speed of the baffled pump and S_{WOB} is the true speed of the unbaffled, as-tested charcoal panel. The baffle transmissivity t, derived from Santeler [12] data, is 0.15 for the two-chevron unit. S_{WOB} is the ratio of the throughout Q to the true pressure P_1 in the cold space.

$$S_{WOB} = \frac{Q}{P_1} = \frac{NT_0}{nT_1}, \tag{5}$$

where N is the throughput particle flow, n is the cold space density and T_0 is the ambient temperature of the incoming helium. The indicated pumping speed (S_{WOBI}) (fig. 15) is based on the gage reading (P_1) in the cold space, which is referenced to ambient temperature, so that

$$S_{WOBI} = \frac{Q}{P_1} = \frac{NT_0}{nT_0} = \frac{N}{n}. \tag{6}$$

The estimated speed of a baffled pump compared to the indicated speed of the panel as tested is then

$$S_{WB} = tS_{WOBI}T_0/T_1. \tag{7}$$

Estimating a cold space temperature of 90 K (shield

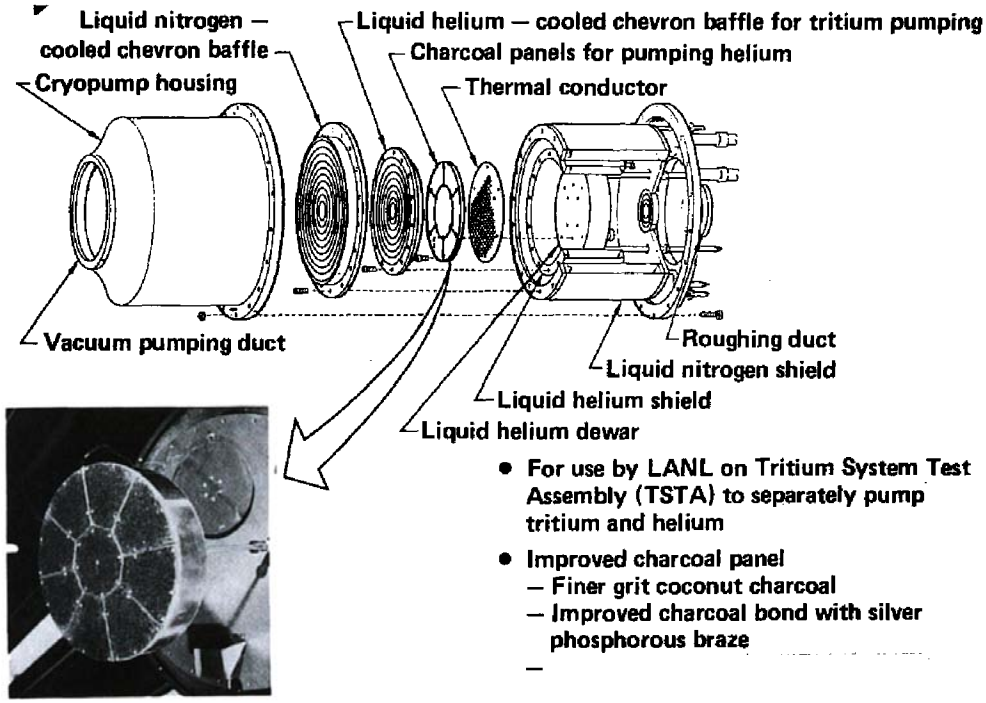

Fig. 14. TSTA upgraded charcoal compound cryopump.

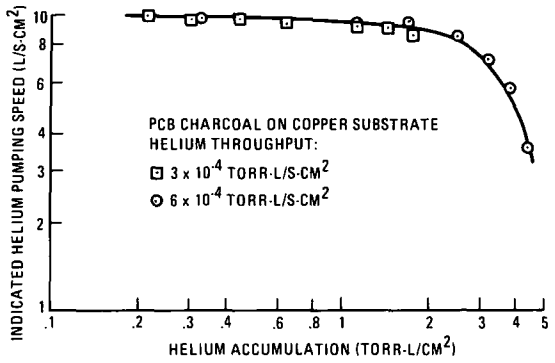

Fig. 15. Helium pumping performance of scaled-up 40-cm diameter charcoal cryopump bonded with 6 mil AgCuP braze.

temperature) and an ambient temperature of 293 K the predicted speed at low helium accumulation for a two-chevron pump is 4.9 $l\ s^{-1}\ cm^{-2}$. Compared to the projection in section 2.2, the predicted result indicates a sticking coefficient of unity for the TSTA panel.

3.5. Charcoal contamination

During performance tests on the 4-inch diameter sample described in section 3.3, wide variations in pumping speed were observed as the charcoal panel exposure in vacuum varied from run to run. Typically, after the sample was tested, and held in the vacuum chamber for several days under vacuum at ambient temperature, subsequent helium pumping performance was measurably reduced. If this deterioration could not be prevented or corrected, then the value of charcoal as a helium cryopump would be diminished greatly.

Samples were prepared to evaluate loss of helium pumping performance. Fig. 16 shows that the performance of the as-received sample vacuum heated at 330 K before cooldown was high. The sample was then kept under vacuum in the chamber for 28-day test duration.

Following the first run the cryogens were purged out of the test pump which was warmed up and remained at ambient temperature under vacuum for five days before being heated again at 330 K. Pumping performance in the second run, dropped below 8.0 $l\ s^{-1}\ cm^{-2}$ compared to 11 $l\ s^{-1}\ cm^{-2}$ for the as-received sample after 20 min of pumping.

The cryogens were purged and the pump allowed to warm up gradually to ambient temperature following the second run. Vacuum was held for an additional 17 days before the sample was heated to 330 K and cooled down for the third run. The helium pumping speed after 20 min at the same helium throughout rate was reduced to approximately 4.5 $l\ s^{-1}\ cm^{-2}$, a 60% decrease compared to the performance of the as-received vacuum-baked sample.

The pump and sample were again allowed to warm to ambient while under vacuum, and held under vacuum for an additional six days. Prior to the fourth run, chevron cooldown with liquid nitrogen and sample bakeout were started. LN cooling was used continuously until completion of the run. Bakeout temperatures were increased to between 380 and 400 K for a 40-hour period. Subsequent helium pumping performance recovered to within 5% of the value attained by the as-received sample in the first run. Subsequent tests showed that samples held in vacuum behind a liquid nitrogen shield between helium pumping runs did not degrade. The potential contaminants in the vacuum chamber such as outgas products from the wall and seals, and condensibles such as water vapor were intercepted by the shield.

3.6. Conclusions of the charcoal study

These results show that braze alloy and copper cement bonding agents meet the requirements to build a charcoal-based fusion-compatible helium cryopump. It was shown that thermal contact between the bonding

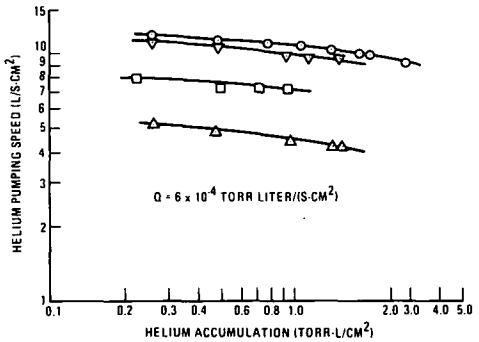

EXPOSURE HISTORY OF CHARCOAL TEST SAMPLES

RUN	AS RECVD	UP TO AIR BEFORE RUN	DAYS UNDER VAC BETWEEN RUNS	LN COOLED BETWEEN RUNS	TEMP OF BAKE (K) BEFORE RUN
○	YES	YES	–	NO	330 - 340
□	NO	NO	5	NO	330 - 340
△	NO	NO	17 (22 CUM)	NO	330 - 340
▽	NO	NO	6 (28 CUM)	YES**	380 - 400 (42.5 HRS)

**LN COOLED DURING DURATION OF BAKE (42.5 HRS)

Fig. 16. Effect of vacuum exposure history on charcoal pumping performance of copper cement bonded charcoal.

agent charcoal and the cryosupport is critical to optimization of the helium pumping performance.

Systems consisting of charcoal bonded with copper cement or braze exceeded the demonstrated capability of a charcoal/epoxy bond standard.

Coconut charcoal in the 12 × 30 mesh size produced the optimum helium pumping performance while coal-based charcoals of this mesh size showed diminished performance.

Repeated or prolonged exposure to vacuum of an ambient temperature sample with no bake or with only low temperature heating resulted in degraded pumping performance. However, surrounding the sample with a thermal shield held at liquid nitrogen temperature during vacuum hold resulted in maintenance of the charcoal's pumping capability. Restoration of pumping performance of degraded charcoal can also be achieved by a 380–400 K bake provided the LN thermal shield is used during the bakeout.

4. Continuous duty cryopump system

In parallel with the development of charcoal sorbent systems for helium cryopumping, a continuous duty cryopump system was developed for fusion applications by Sedgley et al. [16]. The system comprises a self-contained cryopump for in-vessel installation and a microprocessor controller for automatic operation. The pump, designed for pumping deuterium, could be modified readily by addition of charcoal sorbent surfaces to pump helium.

The pump has two units in a single housing, arranged so that one is pumping while the other is regenerating. Liquid helium-cooled, finned sections in each unit pump deuterium by condensation, and an integral collector pump captures the regenerated gas. A microprocessor unit controls distribution of liquid and gaseous helium for conditioning the pumping units and operation of remote actuators for regeneration. Software provides fully automatic, timed sequencing of the repetitive cryopump events.

A unit was developed previously by Batzer [17] for pumping hydrogen (deuterium) which could be immersed in a vacuum chamber for efficient pumping and which cold be regenerated without discharging the previously pumped gas to the vacuum chamber. The unit demonstrated feasibility of the regeneration concept and was prototypical of the unit described here.

The continuous duty cryopump design (fig. 17) evolved from the previously developed regenerable cryopump and retains many of the first pump's proven design features to minimize technology risk. Both pumps feature liquid helium-cooled pumping panels for condensing the deuterium. These panels are provided thermal shielding by a series of Z-shaped double chevrons, with the ends of each zee hinged to its center section (fig. 18). When the hinged portions (louvers) are opened, deuterium passes to the pumping panels from two sides. For regeneration, the pumping surfaces are isolated from the vacuum chamber by closing the hinged portions. Deuterium is dumped from the pumping panels into the cavity formed by the closed louvers by purging the liquid helium coolant. The gas is then pumped from the cavity by an appended collector pump, which is itself a helium-cooled unit. Flow between the pumping units and the collector pump is controlled by doors. The collector pump is regenerated periodically into a roughing system.

Differences between the regenerable pump [17] and the continuous duty cryopump are shown below:

Regeneration – The first pump was not required to demonstrate continuous operation and was therefore regenerated to the collector pump during a shutdown of the pumped gas throughput.

Operation – Control of the first pump's valves and louver actuator was done manually because regeneration was infrequent.

Pumping units – A single pumping unit was sufficient to satisfy the first pump's requirement to demonstrate capability for regeneration. The current pump features two pumping units, so that one unit can be operating while the second is being regenerated.

This two-unit arrangement is prototypical of units that would satisfy a reactor's requirement of continuous operation, but it is not optimum. The pump has 100% excess capacity over that required to satisfy the pumping need. A more appropriate excess capacity would be up to 20% [17] so that a typical reactor installation would feature pumping systems with six individual units capable of sequential regeneration. This arrangement would result in low tritium holdup in a reactor application; for example a maximum of 67 g tritium would be held in the cryopumps of a 3500 MW fusion device [8].

Leaking during regeneration – The first pump was not optimized for minimizing leakage back to the vacuum chamber, and indicated leakage was as high as 30%. The test results showed, however, how the condition could be improved. The current pump features close-fitting louver doors, increased collector pump speed, and increased conductance between the pump units and the collector pump.

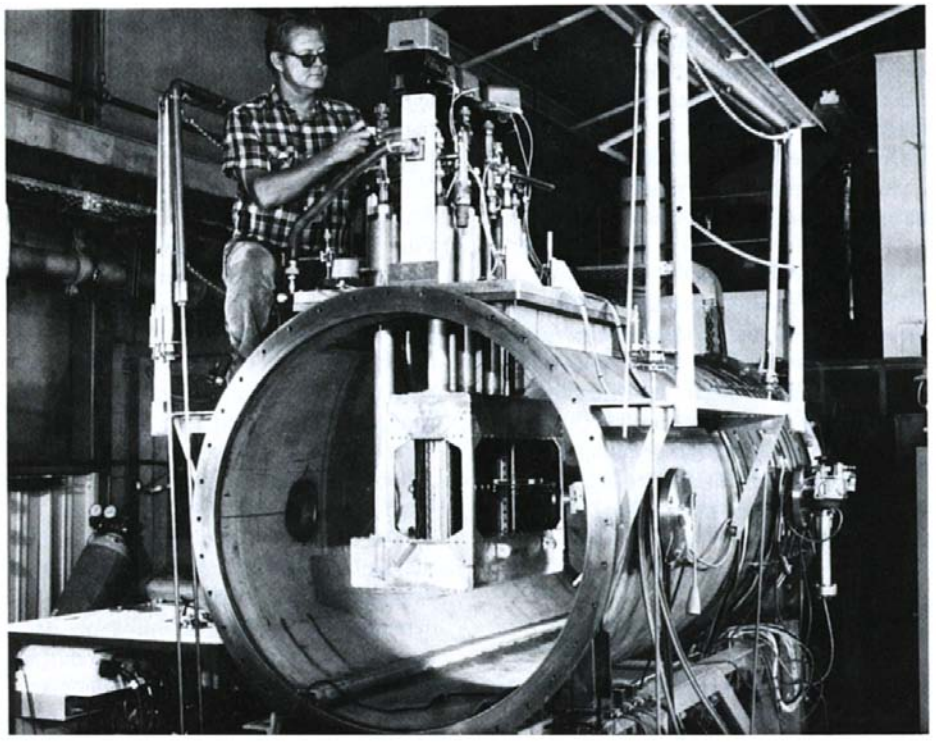

Fig. 17. Continuous duty cryopump installed in test chamber.

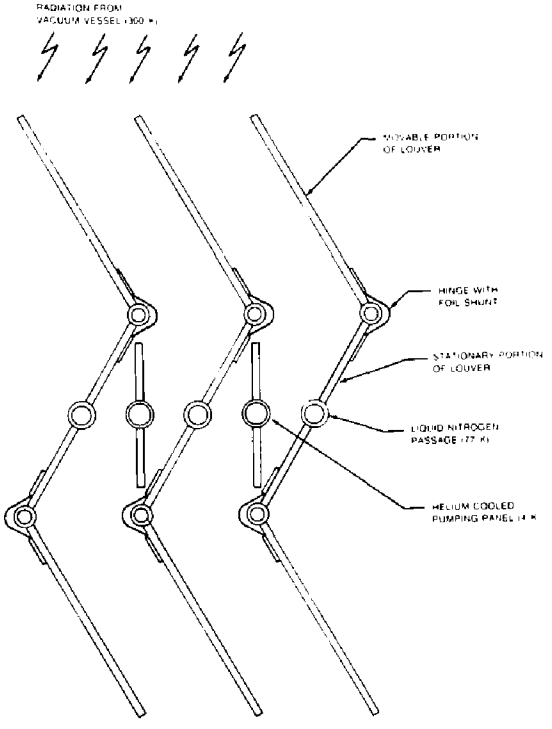

Fig. 18. Arrangement of chevrons in the pump.

4.1. Cryopump

Liquid nitrogen cooled shields, incorporating a hinged, Z-shaped chevron configuration, surround both units. A single mechanism assembly using a driver and reversing link operates all louvers. An integral collector pump (fig. 19) recondenses the pumped gas, evaporated during regeneration. Doors separate each unit from the collector pump. Gas released from the collector pump during its regeneration are pumped by a mechanical roughing system.

The capabilities and characteristics of the cryopump based on design analyses are presented below.

Deuterium speed per unit	12,400 $l\ s^{-1}$
Helium consumption	
– unit regeneration	1 l
– continuous operation	0.4 l/h
Thermal runaway protection	
– time to crack relief	32 s
– max. dewar pressure	0.17 MPa

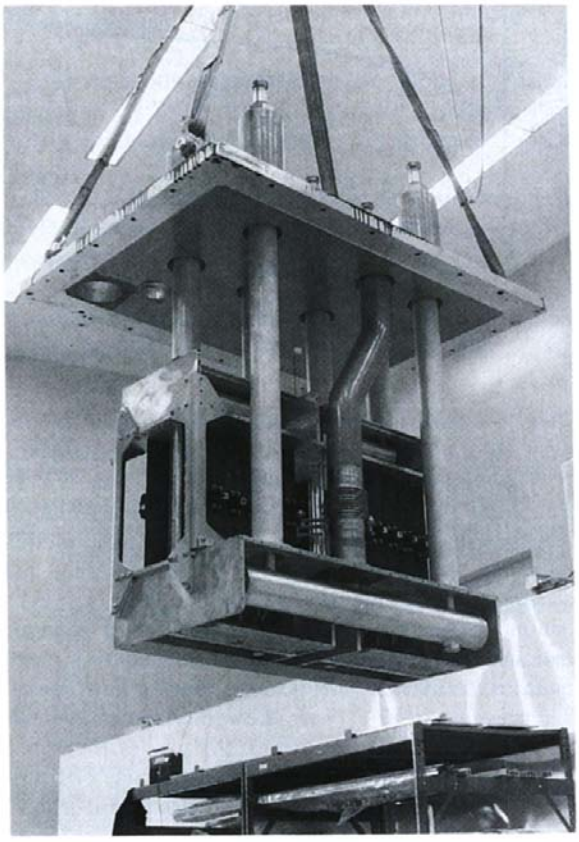

Fig. 19. Partly assembled cryopump showing the collector pump within the lower thermal shield.

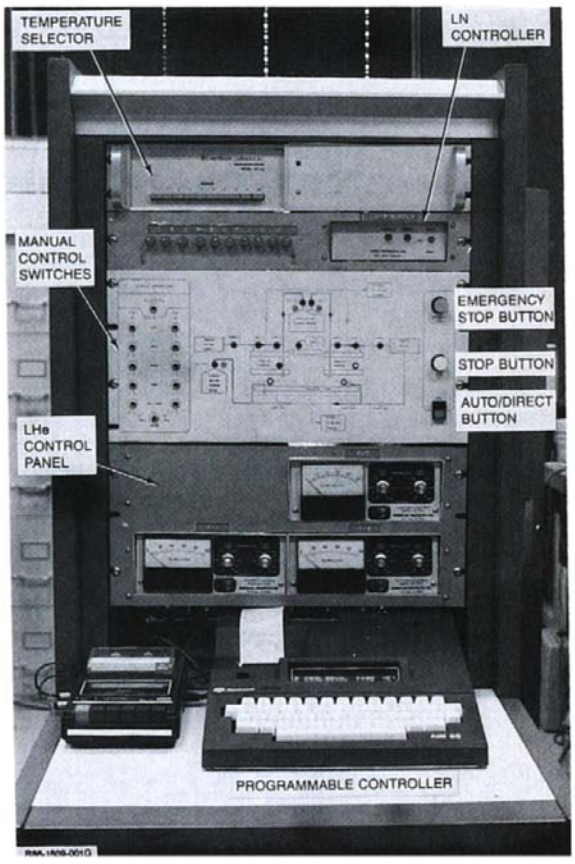

Fig. 20. Cryopump controller.

Leakage back to vacuum chamber during regeneration	6%
Maximum temperature of thermal shield	117 K

4.2. Controller

Control of cryogenic and ambient helium distribution for cooling and warming the pumping units, and operation of remote actuators are performed by a programmable microprocessor unit (fig. 20). Some valves on the collector pump, which is regenerated less frequently than the pumping units, are manually operated. The software provides for fully automatic, timed sequencing of the repetitive cryopump events, which are cooldown, operation and regeneration. Automatic valve commands and timing of the events can be reprogrammed through a keyboard. An override button allows the operator to interrupt automatic operation and to control the helium valves, louvers and collector doors directly through a switch pannel. Temperatures and pressures are monitored, and helium levels within the three pump reservoirs are held automatically.

4.3. Cryopump systems testing

The test program to determine the performance and function of the continuous duty cryopump system was completed at LLNL [18]. The system was initially checked out by using the manual direct mode switches incorporated in the controller. The regeneration and cooldown operations, in which coolant helium was vented and reintroduced to the pump dewars, were verified before exposing the pump to deuterium throughput. Maximum temperature of the liquid nitrogen-cooled shield, including the movable louvers was below 100 K, and liquid helium consumption was below

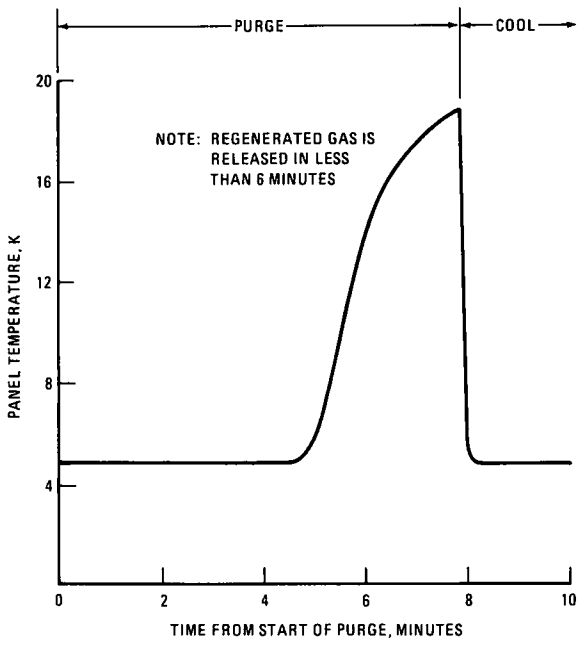

Fig. 21. Typical regeneration (of Panel 1) profile.

expectations. Consumption in the pumping units was limited to the amount purged during each regeneration; no make-up helium was needed during pump operation. A typical temperature profile of a pumping unit during regeneration is shown in fig. 21. The automatic (sequencer) mode was used for continuous periods to test capability.

Pumping speed up to 16,430 $l\ s^{-1}$ was attained. Performance referenced to the pump entrance (fig. 22) exceeded the design speed of 8 $l\ s^{-1}\,cm^{-2}$ deuterium at 10^{-5} Torr (0.124 Torr $l\ s^{-1}\,cm^{-2}$). The conservative analysis of ref. [16] used the conductance of a conventional V-shaped chevron for performance prediction. The trend to lower pumping speed at lower vacuum chamber pressure is indicative of approaching zero pumping equilibrium as chamber pressure approaches deuterium vapor pressure corresponding to the pumping unit's temperature.

Transition of the pump's condition from pumping to regeneration to cooling to pumping was smooth. Back leakage to the 3800 l test vacuum chamber during regeneration was 7.5% of the pump's speed based on data taken with the pump's louvers closed. Although this level is higher than the predicted 6% value, the pressure increase in a reactor installation would be limited to the mid-10^{-5} Torr range. Pressure peaks

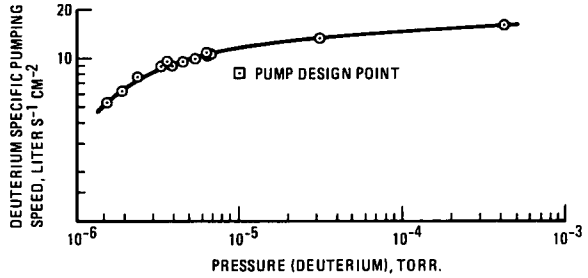

Fig. 22. Deuterium pumping performance of the continuous duty cryopump referenced to pump entrance.

from back leakage to the test chamber measured 4×10^{-4} Torr following regeneration of 180 Torr l (0.12 Torr $l\ cm^{-2}$) of deuterium. However in an operational installation where the ratio of on-line pumping capability would be 5 : 1 compared to 1 : 1 here; and where gas accumulation on the panels is projected to be limited by tritium inventory to less than 0.09 Torr $l\ cm^{-2}$ of pump entrance area, the pressure will be limited to a maximum in the mid-10^{-5} Torr range. Steady state operating pressure is 10^{-5} Torr. Lowering the peak value further would require reducing the gap at the louver seals to less than the test pump's design value of 1 mm. In this dimension range, pressure change is proportional to gap size.

The cryopump system operated continuously in both the direct mode through the switch panel and in the automatic mode with commands issued by the controller software. In each case the pump provided continuous deuterium pumping while it was periodically regenerated.

The pump system which is operational in the LLNL test chamber, can be readily upgraded for helium pumping by addition of charcoal sorbent to its pumping panels.

5. Conclusions

Development of methods for continuously cryopumping the effluents of fusion reactors is well underway. Fusion-compatible sorbent systems consisting of coconut charcoal, attachment bond and substrate have shown helium pumping performance in excess of that of a reference epoxy-bonded charcoal sample. A continuous duty cryopump system has been produced and tested for pumping deuterium. Modification of this unit for pumping helium can be done readily.

Acknowledgment

This work was supported by the Office of Fusion Energy of US DOE through Lawrence Livermore National Laboratory (LLNL) and by Grumman Aerospace Corporation.

The authors wish to acknowledge the contribution of Mr. L. Dietz of Grumman who was instrumental in the program's success.

References

[1] D. Perenic, Kernforschungszentrum Karlsruhe GmbH, personal communication.

[2] T.H. Batzer, R.E. Patrick and W.R. Call, A TSTA compound cryopump, J. Vac. Sci. Technol. 18 (3) (1981) 1125.

[3] H.C. Hseuh, T.S. Chou, H.A. Horwitz and H.J. Halama, Cryosorption pumping of helium by charcoal and a compound cryopump design for TSTA, Proceedings of the 8th Symposium on Engineering Problems of Fusion Research, IEEE Pub. No. 79CH1441-5 NPS.

[4] J.L. Anderson, D.O. Coffin and C.R. Walthers, Vacuum applications for the tritium systems test assembly, J. Vac. Sci. Technol A1(1) (1983).

[5] STARFIRE, a commercial tokamak fusion power study, Argonne National Laboratory, ANL/FPP-80-1.

[6] R.W. Conn, Physics and design of limitors for tokamak experiments and reactors, ANS Sixth Topical Meeting on the Technology of Fusion Energy, San Francisco, 1985.

[7] D.E. Post and R. Mattas, Poloidal divertor systems for impurity and particle control, ANS Sixth Topical Meeting on the Technology of Fusion Energy, 1985.

[8] Mirror Advanced Reactor Study Interim Design Report. Lawrence Livermore National Laboratory, UCRL-53333, (1983) 3–132.

[9] R. Jacobsen, Preliminary particle scoop limiter measurements, Princeton Plasma Physics Laboratory, PPPL-1825 (1981).

[10] D.O. Coffin and C.R. Walthers, Vacuum pumping of tritium in fusion power reactors, Proceedings of the 8th Symposium on Engineering Problems of Fusion Research, IEEE Pub. No. 79CH1441-5 NPS.

[11] J.F. O'Hanlon, A User's Guide to Vacuum Technology (Wiley, New York, 1980) p. 35.

[12] D.J. Santeler et al., Vacuum Technology and Space Simulation, NASA SP-105 (1966).

[13] P.W. Fisher and J.S. Watson, Helium pumping at 4.2 K by molecular sieve 5A, J. Vac. Sci. Technol. 16(1) (1979).

[14] T.H. Batzer and W.R. Call, Mirror fusion vacuum technology developments, Proceedings of the 10th Symposium on Fusion Engineering, IEEE Cat. No. 83CM1916-6 (1983).

[15] D.W. Sedgley, A.G. Tobin, T.H. Batzer and W.R. Call, Development of charcoal sorbents for helium cryopumping, Proceedings of the 10th Symposium on Fusion Engineering, IEEE Cat. No. 83CM1916-6 (1983).

[16] D.W. Sedgley, L.P. Dietz, N.C. Szuchy, T.H. Batzer and W.R. Call, Development of a continuous duty cryopump, American Nuclear Society ANS Sixth Topical Meeting on the Technology of Fusion Energy, San Francisco, 1985.

[17] T.H. Batzer and W.R. Call, A continuous duty cryopump for steady-state mirror reactors, J. Vac. Sci. Technol. (2) (1983) 1315.

[18] D.W. Sedgley, W.R. Call and T.H. Batzer, Cryopumping for fusion power applications, Proceedings of the 11th Symposium on Fusion Engineering, IEEE Cat. No. CH2251-7 (1985).